

Collapsing lattice animals and lattice trees in two dimensions

Hsiao-Ping Hsu and Peter Grassberger

John-von-Neumann Institute for Computing, Forschungszentrum Jülich,
D-52425 Jülich, Germany

E-mail: h.p.hsu@fz-juelich.de and p.grassberger@fz-juelich.de

Received 26 April 2005

Accepted 19 May 2005

Published 6 June 2005

Online at stacks.iop.org/JSTAT/2005/P06003

[doi:10.1088/1742-5468/2005/06/P06003](https://doi.org/10.1088/1742-5468/2005/06/P06003)

Abstract. We present high statistics simulations of weighted lattice bond animals and lattice trees on the square lattice, with fugacities for each non-bonded contact and for each bond between two neighbouring monomers. The simulations are performed using a newly developed sequential sampling method with resampling, very similar to the pruned-enriched Rosenbluth method (PERM) used for linear chain polymers. We determine with high precision the line of second-order transitions from an extended to a collapsed phase in the resulting two-dimensional phase diagram. This line includes critical bond percolation as a multicritical point, and we verify that this point divides the line into different universality classes. One of them corresponds to the collapse driven by contacts and includes the collapse of (weakly embeddable) trees. There is some evidence that the other is subdivided again into two parts with different universality classes. One of these (at the far side from collapsing trees) is bond driven and is represented by the Derrida–Herrmann model of animals having bonds only (no contacts). Between the critical percolation point and this bond-driven collapse seems to be an intermediate regime, whose other end point is a multicritical point P^* where a transition line between two collapsed phases (one bond driven and the other contact driven) sparks off. This point P^* seems to be attractive (in the renormalization group sense) from the side of the intermediate regime, so there are four universality classes on the transition line (collapsing trees, critical percolation, intermediate regime, and Derrida–Herrmann). We obtain very precise estimates for all critical exponents for collapsing trees. It is already harder to estimate the critical exponents for the intermediate regime. Finally, it is very difficult to obtain with our method good estimates of the critical parameters of the Derrida–Herrmann universality class. As regards the bond-driven to contact-driven transition in the collapsed phase, we have some

evidence for its existence and rough location, but no precise estimates of critical exponents.

Keywords: critical exponents and amplitudes (theory), phase diagrams (theory), polymers

ArXiv ePrint: [cond-mat/0504678](https://arxiv.org/abs/cond-mat/0504678)

Contents

1. Introduction	2
2. Numerical methods	5
3. The percolation point	6
4. The region $y < 2$: collapsing trees	8
5. The region $y > 2$	12
6. Collapsed animals: one or two phases?	16
7. Conclusions	18
Acknowledgment	19
References	19

1. Introduction

Lattice animals are just clusters of connected sites on a regular lattice. They play an important role in many models of statistical physics, such as percolation [1] and the Ising model, where they are related to Fortuin–Kastleyn clusters and to the famous Swendsen–Wang algorithm [2, 3]. Apart from this, they also form the prototype model for randomly branched polymers, just as self-avoiding random walks (SAWs) are a model for unbranched polymers [4].

In the case of single unbranched polymers in a very diluted solvent, a much studied phase transition happens when the solvent deteriorates (as it usually does when temperature is lowered). Below the so-called θ -point a polymer no longer forms a swollen coil with Flory radius $R_N \sim N^\nu$ with $\nu > 1/2$ (N is here and in the following the number of monomers), but rather a collapsed ‘globule’ with $R_N \sim N^{1/d}$, where d is the dimensionality of space [5, 6]. In the simplest model of polymers living on a regular lattice, the collapse is induced by an effective attractive interaction between non-bonded monomers on neighbouring lattice sites. It is easy to see that such a monomer–monomer attraction is equivalent to a monomer–solvent repulsion, so there is no need to include the latter, if one is only interested in universal properties of the transition.

A similar collapse transition is expected also to occur for branched polymers. Here the situation is somewhat more complicated, though. In a lattice model, one can introduce two different kinds of attraction, so one obtains a two-dimensional phase diagram with a line of collapse transition points. The basic reason for this difference to unbranched

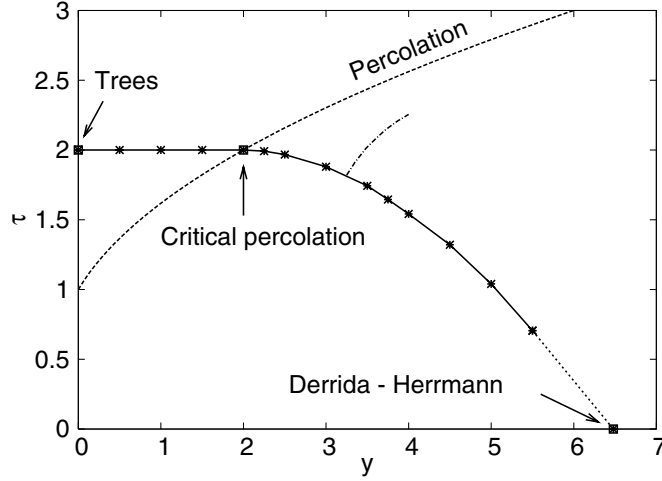


Figure 1. Phase diagram for interacting animals. The full line separates an extended phase (below) from a collapsed phase (above). The points on this line are obtained by Monte Carlo simulations in the present work, except for the point at $y = 6.48, \tau = 0$ which is taken from [16]. At $y = 0$ the clusters are trees (minimal number of bonds), while at $\tau = 0$ they have no contacts but only bonds. The dashed line corresponds to bond percolation, with the critical point being at $y = \tau = 2$. The short dashed-dotted line is a rough estimate for the transition between a contact-rich and a bond-rich collapsed phase.

polymers (interacting self-avoiding walks, ISAWs) is that the number of bonds is fixed to $b = N - 1$ for SAWs (as it is also for trees), while it can fluctuate, $b \geq N - 1$, for general animals. Thus one can introduce two different fugacities for monomer–monomer bonds and for non-bonded monomer–monomer contacts. As for unbranched polymers, there is no need to introduce a separate monomer–solvent interaction, since the number s of monomer–solvent contacts is not independent, but is given by

$$\mathcal{N}N = 2b + 2k + s, \quad (1)$$

where \mathcal{N} is the lattice coordination number ($\mathcal{N} = 2d$ on a simple hypercubic lattice in d dimensions) and k is the number of non-bonded monomer–monomer contacts. A general partition sum for interacting lattice animals is therefore [7]–[15]

$$Z_N(y, \tau) = \sum_{b,k} C_{Nbk} y^{b-N+1} \tau^k, \quad (2)$$

where C_{Nbk} is just the number of configurations (up to translations and rotations) of connected clusters with N sites, b bonds, and k contacts. Notice that we changed the definition slightly with respect to [7]–[15], so that $Z_N(y, \tau)$ is non-zero for $y = 0$.

The phase diagram in terms of the control parameters y and τ is shown in figure 1 for two-dimensional animals on the square lattice. There is an extended phase for small y and τ which includes also the unweighted animal model ($y = \tau = 1$), and at least one collapsed phase. At the collapse transition we expect that

$$Z_N(y, \tau = \tau_c(y)) \sim \mu(y)^N N^{-\theta}, \quad (3)$$

where $\mu(y)$ should depend continuously on y , but θ should take discrete values depending on the respective universality class.

There have been claims, based on exact enumerations of very small clusters [9, 10], that there are two distinct collapsed phases, one bond rich and the other contact rich. This has led to some controversy, since later authors could not find it either with other numerical models [8] or in simplified models [7]. We also find such a transition between two collapsed phases, although at significantly smaller values of y (short dashed-dotted curve). The two end points of the transition curve shown in figure 1 are given by collapsing weakly embeddable trees ($y = 0$) and by a model where non-bonded contacts are forbidden ($\tau = 0$). The latter has been studied in detail by Derrida and Herrmann [16], and others [17]–[20].

Bond percolation is a special model of weighted clusters. The generating function for bond percolation clusters is defined as

$$Z_N^{\text{perc}}(p) = \sum_{b,k} C_{Nbk} p^b (1-p)^{k+s}. \quad (4)$$

More precisely, this equation gives the probability that the origin is connected to a cluster of precisely N sites, if lattice bonds are established with probability p and broken with probability $1-p$. Using equation (1), one sees that

$$Z_N^{\text{perc}}(p) = (1-p)^{\mathcal{N}N-2N+2} p^{N-1} Z_N(y(p), \tau(p)), \quad (5)$$

with the curve $(y(p), \tau(p))$ parameterized as

$$y = p/(1-p)^2, \quad \tau = 1/(1-p), \quad 0 \leq p \leq 1 \quad (6)$$

or given explicitly by

$$y = \tau(\tau - 1). \quad (7)$$

This curve is also shown in figure 1. It contains in particular the critical bond percolation point, $p = 1/2$, corresponding to $y = \tau = 2$. This point lies also on the collapse transition line [7], and divides it into two parts: one branch with high density of contacts ($y < 2$) and one with high density of bonds ($y > 2$). Since it is known that the critical percolation point is fully repulsive in the renormalization group (RG) sense [21], it would be natural to assume that the RG flow along the transition curve goes to the two end points $y = 0$ (collapsing trees) resp. $\tau = 0$ (Derrida–Herrmann model). Thus we could naively expect that the critical behaviour on each of the two parts of the transition curve is given by the fixed point at its end. But if there are indeed two different collapsed phases, then the point at which the transition line between them meets the collapse transition line should be some multicritical point (y^*, τ^*) . *A priori*, this point could be the critical percolation point. But according to [9, 10, 22] this is clearly not the case: while $y = 2$ for percolation, $y^* \approx 4$ (see figure 2 of [7]). If all that is true, then there should be two multicritical points on the transition curve, and three different universality classes in addition to the percolation class.

In the following we shall investigate the details of this scenario by means of extensive Monte Carlo simulations. In section 2 we shall briefly describe the algorithm. The critical percolation point is studied in section 3, both as a means to verify the exactness of our codes and to discuss the crossover exponents at this point. We shall see that both crossover

exponents (the one associated to fluctuations of the number of bonds and the other one for contacts) are exactly equal to $1/2$, although the fluctuations of the number of contacts have huge corrections to scaling. After that we turn in section 4 to the collapse of trees, i.e., to the case $y < 2$. We find that there our results are very clean, allowing us to obtain conjectures for the exact values of all critical exponents. We also verify with high precision a previous conjecture that the transition curve for $y < 2$ is strictly horizontal, with $\tau = 2$. Next, we will turn to the case $y > 2$ in section 5. There we have many more problems in arriving at a consistent scenario, presumably because there exist indeed two different collapsed phases which meet on the transition curve at a point different from critical percolation. In particular, at face value our results would suggest that the crossover exponent for bonds depends continuously on y , and would thus be not universal. But apart from these problems it seems very clear that the critical behaviour for $y > 2$ is not in the same universality class as that for $y < 2$, in contrast to recent speculations [14]. We follow up the question of a transition between two collapsed phases by simulating deep in the collapsed phase. We conclude with a discussion in section 7.

2. Numerical methods

We use essentially the same method as in [23]. There we introduced a sequential sampling method with resampling, implemented depth-first as in the PERM (pruned-enriched Rosenbluth method) algorithm of [24]. More precisely, we first choose a value of p near the percolation threshold (i.e., $p \approx 1/2$), and simulate bond percolation clusters at this p by means of a variant of the Leath algorithm [25]. While they are still growing we estimate their current contribution to the percolation partition sum, and—by reweighting them according to the animal ensemble, equation (2)—to the animal ensemble. If the latter happens to be higher than average, we clone the cluster and let both copies evolve independently further. If the weight is too small, we prune with probability $1/2$ and increase the weights of the survivors by a factor 2.

For this to be efficient, we have to take the following considerations into account.

- The clusters are grown breadth first, not depth first [23], although the ‘population control’ is done depth first.
- The optimal value of p depends on y and τ , and has to be found by trial and error.
- The optimal value of the pruning/cloning threshold was found, to very good precision, to be the same as for ordinary animals [23], although we could improve also this by trial and error search.
- To make things even more subtle, the optimal parameters depended slightly on the maximal sizes to be simulated.

To monitor the performance of the algorithm, we used mostly the variance of the estimated partition sum. Notice that estimating the partition sum is an integral part of this algorithm (it is needed for the ‘population control’). In addition, we checked that the distributions of ‘tour weights’ remain acceptable, as described in [23].

It is clear that this algorithm should work best near the percolation point (since there is then a minimal amount of resampling needed). Indeed, exactly at the percolation point the method works even better than Leath itself, if one uses p slightly below $1/2$. The

reason is that with $p = 1/2$ and without resampling the sample contains very few large but finite clusters. The partition sum equation (4) decreases at $p = p_c = 1/2$ very slowly with N , like $N^{-0.054945}$ [1]. Thus most clusters which did not stop growing early will do so only very late, beyond the maximal N we can simulate. Therefore, estimates of specific heat or of gyration radii will be based on rather small samples and will have rather large errors. With resampling we can work at $p < p_c$, and we will have many more large finished clusters in the sample.

All the work reported in this paper was done on fast Linux PCs and used nearly two years of CPU time.

3. The percolation point

We use the above algorithm to simulate critical bond percolation clusters ($y = \tau = 2, p = 1/2$) of up to $N = 6000$ sites. The nominal p -value at which the clusters were grown was $p \approx 0.473$, the difference between this and the target value $p = 1/2$ being made up by reweighting. In this way the variances of the observables were reduced by roughly two orders of magnitude, as compared to a straightforward Leath algorithm.

Results for the logarithm of the partition sum and for the gyration radius will be shown later, together with results obtained for $y < 2$. They will be discussed in detail in the next section; here we just point out that they are in perfect agreement with the expectations [1]

$$Z_N^{\text{perc}}(p = 1/2) \sim N^{-5/91}, \quad R_N^2 \sim N^{96/91} \quad (8)$$

and with simulations using the plain Leath algorithm.

More interesting are the average numbers of contacts and bonds, and the fluctuations thereof. Near the critical point, one has the scaling ansatz [1]

$$Z_N^{\text{perc}}(p) \approx N^{-5/91} F((p - 1/2)N^\sigma) \quad (9)$$

with $\sigma = 36/91$. This gives $\partial \ln Z_N^{\text{perc}} / \partial p|_{p=1/2} \sim N^\sigma$ and $\partial^2 \ln Z_N^{\text{perc}} / \partial p^2|_{p=1/2} \sim N^{2\sigma}$. On the other hand, using the defining equation (3), one obtains at $p = 1/2$

$$\left. \frac{\partial \ln Z_N^{\text{perc}}}{\partial p} \right|_{p=1/2} = \frac{1}{2} \langle b - s - k \rangle \quad (10)$$

and

$$\left. \frac{\partial^2 \ln Z_N^{\text{perc}}}{\partial p^2} \right|_{p=1/2} = \frac{1}{4} \{ \text{Var}[b - s - k] - \langle b + s + k \rangle \}. \quad (11)$$

Using this and eliminating s in favour of N , one finds that

$$\langle 3b + k \rangle = 4N + O(N^\sigma), \quad (12)$$

while

$$\text{Var}[3b + k] = 2\langle b \rangle + O(N^{2\sigma}). \quad (13)$$

Our estimates for the average numbers of bonds and contacts are

$$\langle b \rangle = 1.1215(3)N + O(N^\sigma), \quad \langle k \rangle = 0.6360(5)N + O(N^\sigma), \quad (14)$$

in excellent agreement with equation (12).

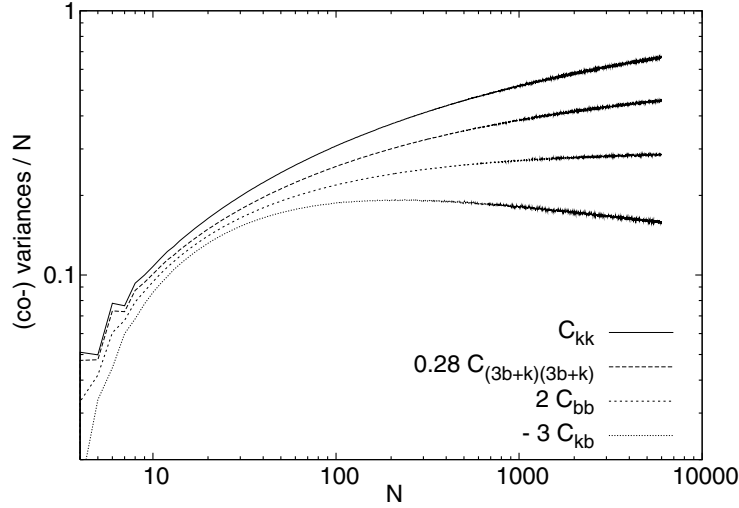


Figure 2. Variances and covariance for bond and contact numbers at the critical percolation point, divided by N . Normalizations are chosen such that the curves do not overlap. Notice that the covariance is negative for all N and increases less quickly than N . In contrast, all three variances increase asymptotically $\sim N$, although with vastly different finite size corrections.

Our results for the 2×2 covariance matrix of the bond and contact numbers are shown in figure 2. More precisely, we show there the (co-)variances divided by N ,

$$C_{ij} = (\langle ij \rangle - \langle i \rangle \langle j \rangle) / N. \quad (15)$$

From this figure we see first that C_{bk} is negative for all N . This is intuitively very plausible: the sum $b+k$ fluctuates less than b and k themselves. Moreover, C_{bk} seems to scale as N^α with $\alpha \approx -0.09$, i.e., the covariance between bonds and contacts increases less fast than N . Secondly, we see that C_{bb} tends to a constant for $N \rightarrow \infty$. A more precise analysis shows that the corrections to this are $\propto N^{-1/2}$, i.e., $C_{bb} \sim (1 - \text{const}/N^{1/2})$. Next, the variance of $3b+k$ seems to scale with a power of N larger than 1, but this would contradict equation (13). Indeed, a more careful analysis shows that the data for $\text{Var}[3b+k]$ are in perfect agreement with equation (13), and that the increase apparent of $\text{Var}[3b+k]/N$ with N is entirely due to the (predicted!) corrections to scaling. Finally, although it increases even faster with N , $\text{Var}[k]$ must also ultimately scale $\sim N$, since it is just a linear combination of the previous (co-)variances.

We should stress again that all these results are as expected from the scaling theory for percolation (although they had not been derived or checked previously, to our knowledge¹). They show that naive power law fits without guidance by the scaling theory would lead to $C_{kk} \sim N^\beta$ with $\beta > 0$ and thus to erroneous conclusions.

¹ For critical site percolation one has $\langle s \rangle = (1 - p_c)N/p_c + O(N^\sigma)$ and $\text{Var}[s] = (1 - p_c)N/p_c^2 + O(N^{2\sigma})$, where s is the number of non-wetted perimeter sites and $p_c = 0.5927 \dots$. The only paper dealing with fluctuations of bonds, contacts, or perimeter sites in percolation we are aware of is [26], but these authors were unaware of the fact that these fluctuations could be derived from accepted scaling ansatz.

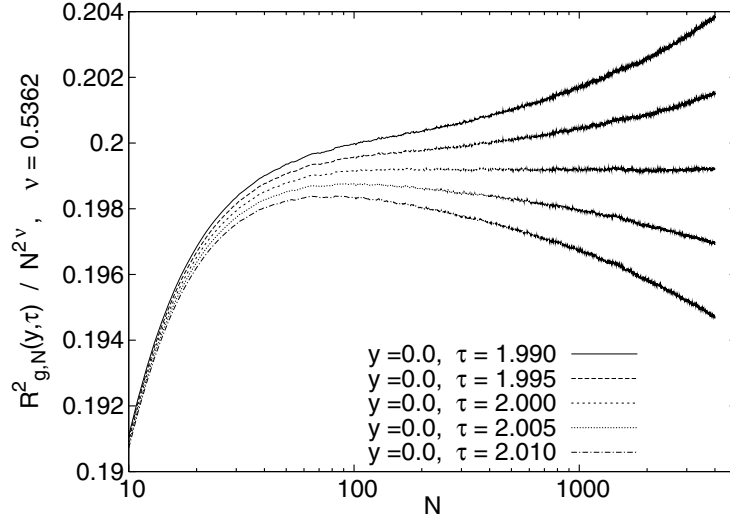


Figure 3. $R_N^2/N^{2\nu}$ for $y = 0$ and for five values of τ close to $\tau = 2$, plotted against $\ln N$. The Flory exponent used for this plot was $\nu = 0.5362$.

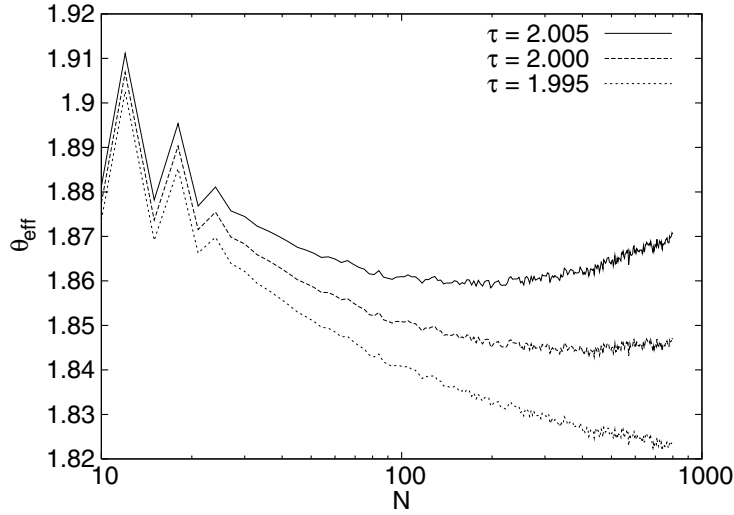


Figure 4. Effective θ -exponents, defined by equation (16), plotted against $\ln N$.

4. The region $y < 2$: collapsing trees

Let us first discuss the case $y = 0$, and treat the general case $0 < y < 2$ later. In this case there are only the minimal number of bonds, $b = N - 1$. To find the transition point $\tau_c = \tau_c(0)$, we studied the scaling of the gyration radius and of the partition sum. We also studied the specific heat (i.e., the variance of the number of contacts), but as in previous cases [23, 28] this gives much less precise estimates.

In figure 3 we plot the rescaled squared gyration radii, $R_N^2/N^{2\nu}$, with a suitably chosen value of ν , against $\ln N$. In figure 4 we show effective exponents θ_{eff} defined by the triple

Table 1. Estimates of critical points $\tau_c(y)$, of critical exponents ν and θ , and of inverse critical fugacities $\mu(y)$.

y	$\tau_c(y)$	ν	θ	$\mu(y)$
0.0	2.0	0.5362(1)	1.845(1)	7.148 93(2)
0.5	2.0	0.5362(1)	1.845(1)	7.3432(1)
1.0	2.0	0.5362(1)	1.845(1)	7.5485(1)
1.5	2.0	0.5362(1)	1.845(1)	7.7665(2)
2.0	2.0	0.527 47...	2.054 94...	8.0
2.25	1.994(2)	0.5230(12)	2.11(1)	8.1088(5)
2.5	1.970(4)	0.5223(8)	2.12(1)	8.1770(5)
3.0	1.880(3)	0.5220(4)	2.12(1)	8.2275(5)
3.5	1.733(7)	<0.524	<2.05	8.182(3)
3.75	1.642(6)	0.524(2)	<2.03	8.109(5)
4.0	1.54(1)	0.524(2)	2.00(3)	8.035(10)
4.5	1.32(1)	0.520(3)	2.01(4)	7.88(2)
5.0	1.04(1)	0.521(3)	1.98(5)	7.63(3)
5.5	0.71(1)	0.522(4)	1.88(6)	7.32(4)

ratios [27]

$$\theta_{\text{eff}}(N, \tau) = \frac{7 \ln Z_N - 6 \ln Z_{N/3} - \ln Z_{5N}}{6 \ln 3 - \ln 5}. \quad (16)$$

If we assume the scaling ansatz

$$Z_N(y, \tau) \sim \mu(y)^N N^{-\theta} G((\tau - \tau_c(y))N^\phi), \quad (17)$$

these triple ratios should tend to θ for $N \rightarrow \infty$, provided $\tau = \tau_c(y)$.

From these plots we obtain $\tau_c(y=0) = 2.001 \pm 0.001$ (from figure 3) and 1.998 ± 0.002 (from figure 4). We conjecture that the collapse transition occurs indeed exactly at $\tau_c = 2$. This was already conjectured by previous authors [13], although based on much more noisy data. Our best unbiased estimates of the critical exponents for collapsing trees are

$$\nu = 0.5359 \pm 0.0003, \quad \theta = 1.842 \pm 0.002. \quad (18)$$

If we accept the conjecture that $\tau_c = 2$, then these estimates can be improved to

$$\nu = 0.5362 \pm 0.0001, \quad \theta = 1.845 \pm 0.001. \quad (19)$$

These values are close to rationals with relatively small denominators, which might suggest that ν and θ are indeed simple rational numbers, $\nu = 37/69 = 0.536 23 \dots$ and $\theta = 59/32 = 1.843 75$. Together with the estimated inverse critical fugacity and with results given below, these estimates are collected in table 1.

Universality suggests that the same exponents should also describe the transition for all $y < 2$. But direct verification is less easy, since there are important corrections to scaling due to the crossover from the percolation point. Making plots like figures 3 and 4 for $y > 0$ would not give very clean results: searching for cleanest power laws would give exponents which depend on y , and would give mutually exclusive estimates $\tau_c(y)$ from the gyration radius and from the partition sum scaling.

We therefore adopt a different strategy. Assuming that $\tau_c(y) = 2$ for all $y \leq 2$ and that critical exponents are independent of y , we plotted in figure 5 $R_N^2/N^{2\nu}$ against N

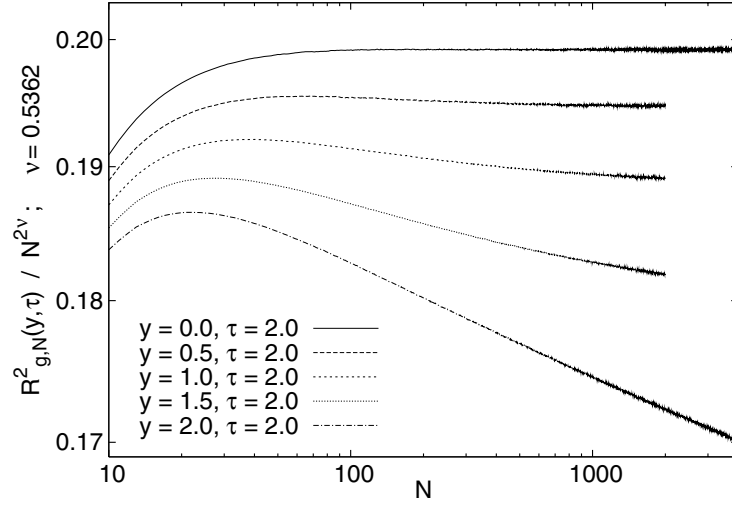


Figure 5. Log-log plot of $R_N^2/N^{2\nu}$ for $\tau = 2$ and for five values of y (0.0, 0.5, 1.0, 1.5, and 2.0). The Flory exponent used for this plot was $\nu = 0.5362$ as obtained from figure 3.

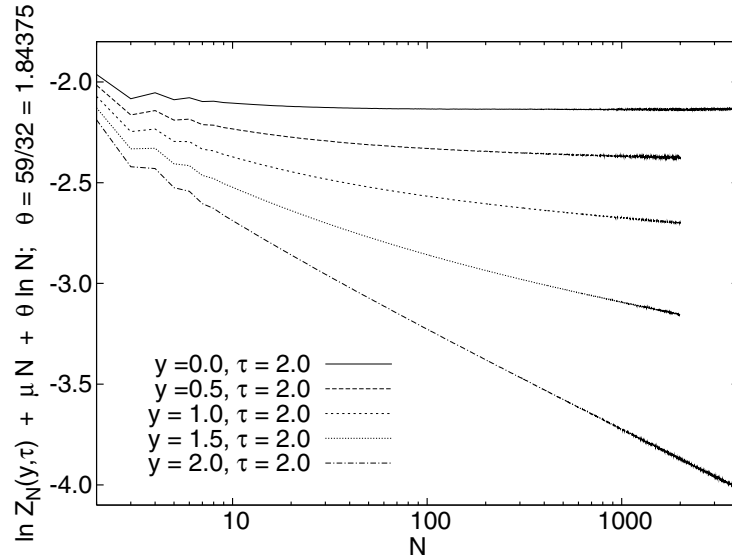


Figure 6. Values of $\ln[Z_N N^\theta / \mu(y)^N]$ for $\tau = 2$ and for the same five values of y as used in figure 5. The value of θ is that for $y = 0$. The critical inverse fugacities $\mu(y)$ were chosen such that the curves show least bending for large N .

for different values of y . Similarly, we plotted $\ln[Z_N N^\theta / \mu(y)^N]$ in figure 6, where $\mu(y)$ is carefully chosen such as to take into account the dominant exponential increase of $\ln Z_N$ with N . In both plots, the curves for percolation (i.e., the lowermost curves) become straight lines for $N \rightarrow \infty$, with slopes $2(\nu^{\text{perc}} - \nu^{\text{tree}})$ and $\theta^{\text{tree}} - \theta^{\text{perc}}$ (notice that θ^{perc} is usually called τ in the percolation literature [1]). The curves for trees ($y = 0$) become horizontal. Finally, the curves for $0 < y < 2$ first follow the percolation curves and ultimately also become horizontal for $N \rightarrow \infty$, but very slowly due to the slow crossover.

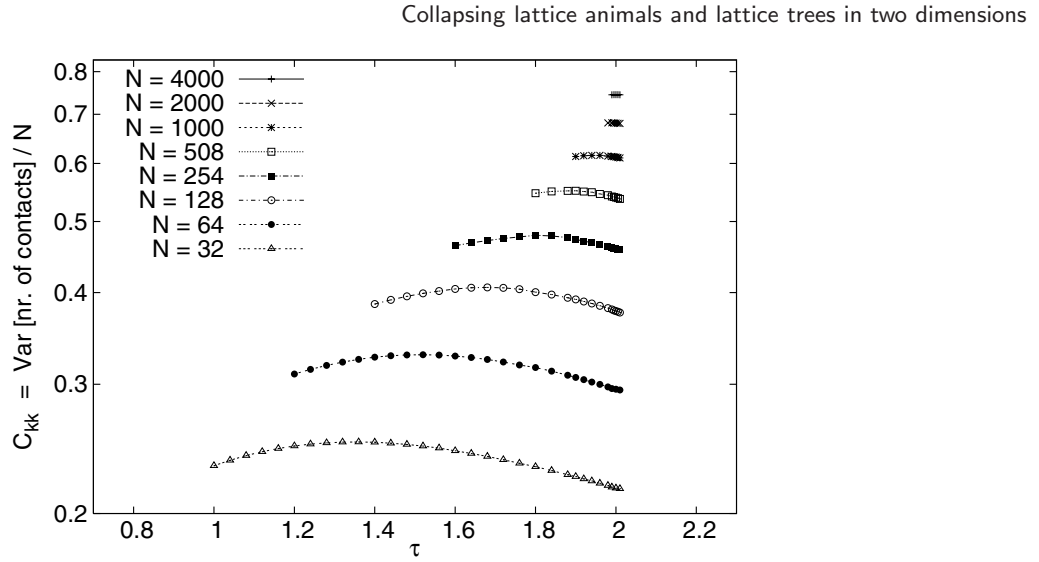


Figure 7. Variances of contact numbers divided by N , plotted against τ , for $y = 0$ and for various values of N .

Although we cannot claim from figures 5 and 6 that this scenario is unique, they strongly suggest that there is indeed just a slow crossover from critical percolation to collapsing trees, and that the collapse transition occurs for all $y < 2$ exactly at $\tau = 2$.

Let us finally discuss the fluctuations of the bond and contact numbers. The normalized variance of the number of contacts, C_{kk} , of collapsing trees (i.e., at $y = 0$) is shown in figure 7 as a function of τ for various values of N . These data are in good agreement with the less precise results of previous simulations [12, 14]. They verify that $\tau_c(0) \approx 2$, but it would obviously be difficult to estimate from them $\tau_c(0)$ (as attempted in [12, 14]) with a precision comparable to that obtained from figures 3 and 4.

Fluctuations for different values of y but precisely at $\tau = \tau_c(y)$ are shown in figures 8–10. In each figure, the normalized (co-)variance is plotted against $\ln N$. For $y \leq 2$ the curves correspond to $\tau = 2$, while they represent our best estimates of the collapse transition for $y > 2$.

As expected, the fluctuations of b are very small and tend to zero as $y \rightarrow 0$. They scale $\sim N$. The bond-contact covariances seem to increase more slowly than N for all $y > 0$, although the decrease of $|C_{bk}|$ with increasing N becomes weaker for small y . Of most interest (for the present case $y < 2$) is the scaling of C_{kk} , since it is the contacts which should drive the collapse transition.

Obviously C_{kk} increases with N . Naive fits (e.g. least square) would give power laws $C_{kk} \sim N^{2\phi-1}$ with $\phi \approx 0.6$ to 0.65 . This would agree with previous estimates [8, 9], [12]–[14], but we should be extremely careful with accepting such a fit. The reason is that there is no qualitative difference between the cases $y < 2$ and $y = 2$, and for the latter we had seen in section 3 that $C_{kk} \rightarrow \text{const}$ for $N \rightarrow \infty$. Thus we propose that $C_{kk} \rightarrow \text{const}$, i.e., $\phi = 1/2$, also for $y < 2$. If we would have $\phi > 1/2$, then there should be either a clear crossover (which is not seen in figure 10), or ϕ would have to be non-universal.

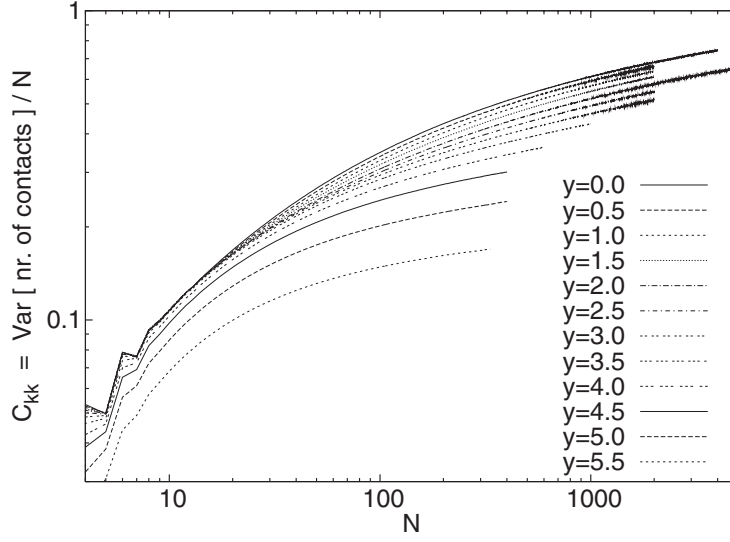


Figure 8. Variances of contact numbers divided by N , plotted against $\ln N$. For each y the curve is for our best estimate of $\tau_c(y)$.

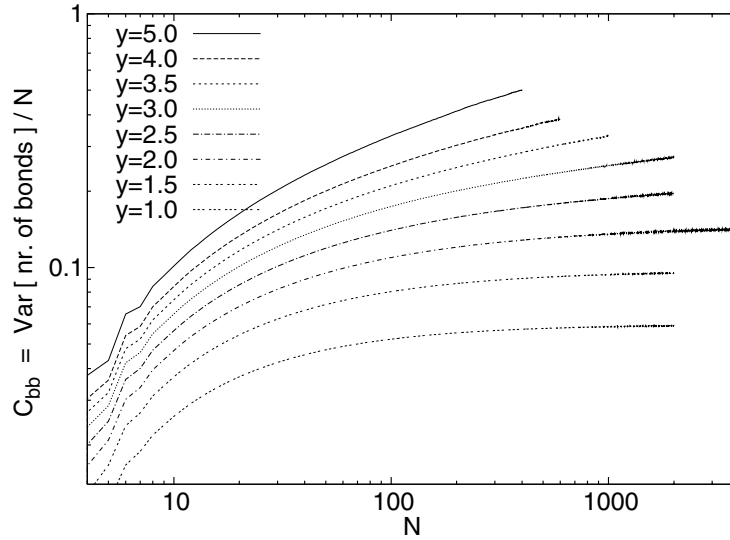


Figure 9. Same as figure 8, but for number of bonds.

5. The region $y > 2$

For $y > 2$ the clusters are richer in bonds, and less rich in contacts. The collapse transition was again located by requiring both the gyration radius and the partition sum to scale. But this time it is much more difficult to estimate corrections to scaling. The main reason is that our algorithm deteriorates very rapidly when y becomes large. While it is still efficient for $y \leq 3.5$, it becomes virtually useless for $y \geq 5.5$. According to [16], the end point of the transition line is at $y = y_{DH} = 6.48 \pm 0.12$. At this point, the present algorithm was unable to give reasonable statistics of clusters with $N = 200$. The algorithm based on

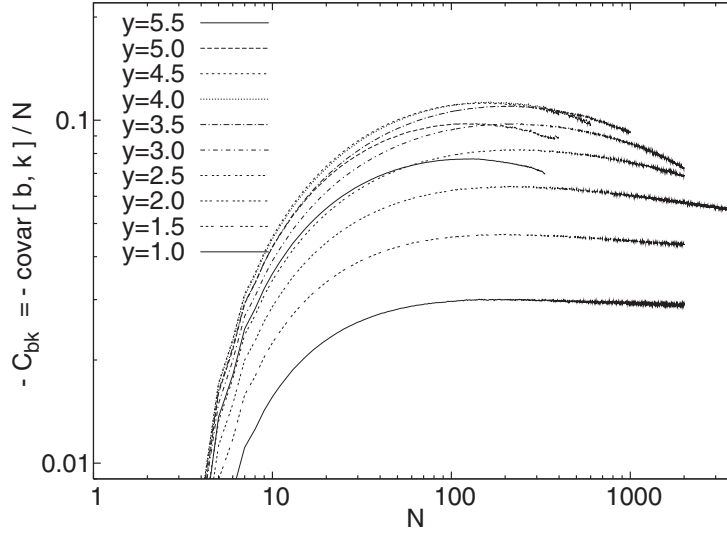


Figure 10. Similar to figures 8 and 9, but for the covariances between bond and contact numbers. Since these covariances are negative for all y and N , we actually plot $-C_{bk}$.

site animals discussed in [23] does a bit better and allowed us to obtain a good sample of clusters with $N = 300$. But even for this sample errors are quite large, and extrapolation to $N \rightarrow \infty$ obviously becomes very difficult. We thus do not present any data for the Derrida–Herrmann model ($\tau = 0, y = y_{DH}$), but we just state that our simulations were in complete agreement with the results of [16].

We therefore must obtain estimates of the critical parameters from the region $2 < y < 5$, although there could again be important crossover contributions from the percolation point.

Typical results for $y = 3.0$ are shown in figures 11 and 12. In figure 11 we see that gyration radii suggest the transition to be at $\tau_c(y = 3.0) = 1.878 \pm 0.003$, with $\nu = 0.5222 \pm 0.0005$. Effective θ -exponents defined by equation (16) are shown in figure 12. They corroborate the determination of τ_c ; more precisely, they suggest $\tau_c(y = 3.0) = 1.884 \pm 0.004$. Using as a compromise $\tau_c(y = 3.0) = 1.880 \pm 0.003$, we obtain as our best estimates of the critical exponents $\nu = 0.5220 \pm 0.0004$ and $\theta = 2.12 \pm 0.01$.

Estimates of ν and θ compatible with these were obtained for $y = 2.5$ and 2.25 , with $\tau_c(y = 2.5) = 1.970 \pm 0.004$ and $\tau_c(y = 2.25) = 1.994 \pm 0.002$. But we encountered problems when going to $3.5 \leq y \leq 4$. Results analogous to figures 11 and 12, but for $y = 3.75$, are shown in figures 13 and 14. This time, there is no value of τ at which R_N^2 shows a pure power law for large N (say, $N > 100$). For small τ the curves bend upward (the clusters are extended), while for $\tau \geq 1.630$ they bend down for very large N , showing that the collapse sets first in for very large clusters only. Moreover, taking the curve in figure 13 for $\tau = 1.625$ (which seems to become straight for very large N) to estimate ν , we would obtain $\nu = 0.527$, which is definitely much larger than the estimates obtained from $2.5 \leq y \leq 3.0$.

Similarly, the partition sum also shows late scaling, with all curves in figure 14 decreasing. Only the curves for $\tau \geq 1.64$ show some tendency to level off for very large

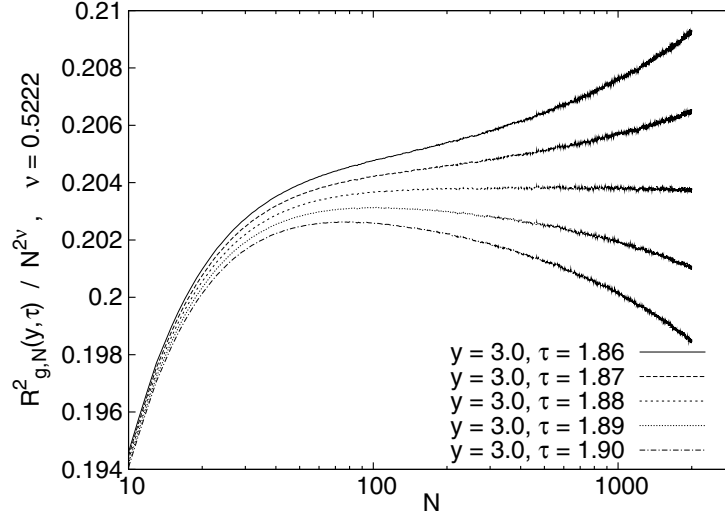


Figure 11. Average squared gyration radii for $y = 3.0$, divided by $N^{1.044}$ and plotted against $\ln N$.

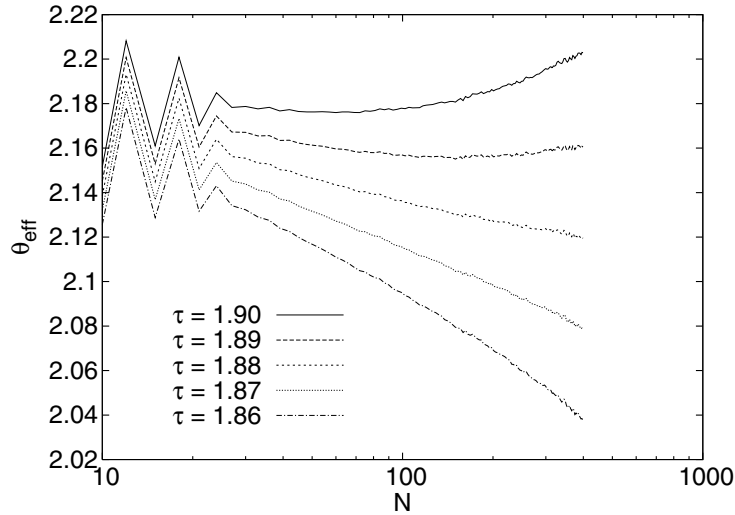


Figure 12. Effective exponents θ_{eff} at $y = 3.0$, plotted against $\ln N$.

N . If this is taken as an indication that scaling should set in similarly late also for the gyration radii, then indeed the lowest curve in figure 13 should be the critical one, and its slope for $N > 1000$ should give the correct estimate of ν : $\nu \approx 0.520$. But all this looks very unconvincing. In addition, the value of θ suggested from figure 14 is much smaller than that from figure 12, any reasonable estimate based on figure 14 being $\theta \leq 2.06$.

Similar results were obtained for $y = 3.5$ and 4.0 . In all these cases the estimated value of θ is definitely smaller than the estimate obtained from $y = 2.5$ and 3.0 . Our best estimates from the region $y \geq 3.5$ are $\theta < 2.0$, $\nu < 0.515$. Notice that this is not easily understood from a crossover from percolation, since there $\theta = 187/91 = 2.054945$. Why

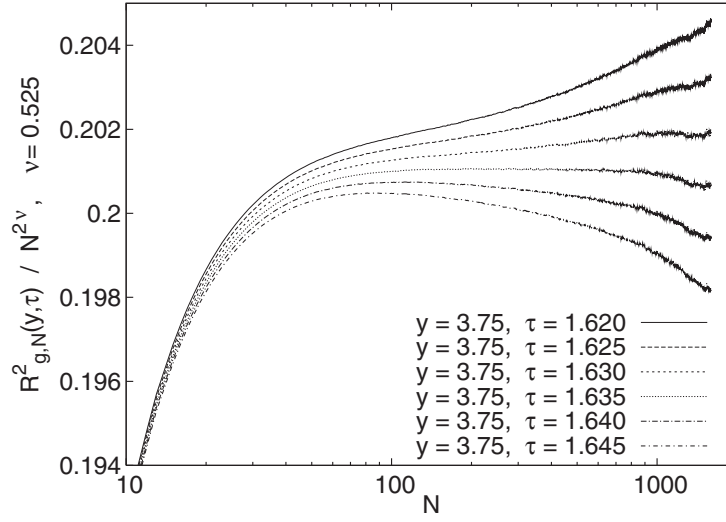


Figure 13. Average squared gyration radii for $y = 3.75$, divided by $N^{1.05}$ and plotted against $\ln N$.

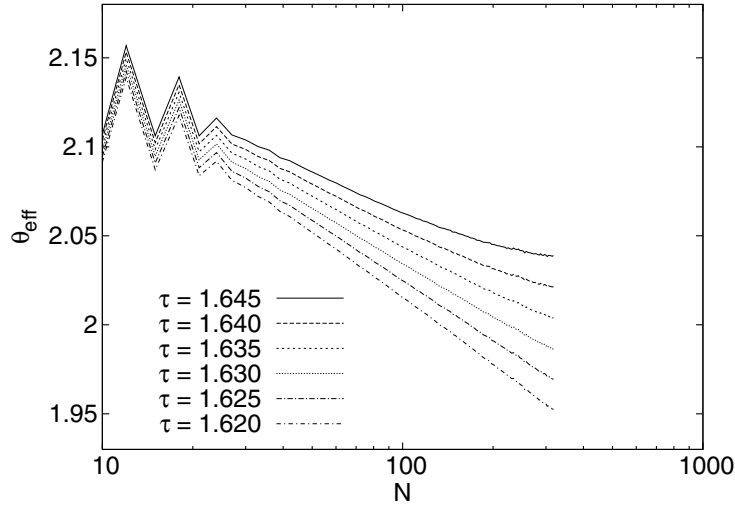


Figure 14. Effective exponents θ_{eff} at $y = 3.75$, plotted against $\ln N$.

should the estimates first move away from the percolation value as we move away from the percolation point, just to come back to it later?

Notice that these difficulties, serious as they are for the estimation of the critical exponents, have very little effect on the estimation of $\tau_c(y)$. In spite of them, our estimates (shown in figure 1) have errors less than 0.02.

They also have very little influence on the estimates of the bond and contact variances. These depend rather weakly on τ (thus they would not be very useful for determining the collapse transition curve, as proposed in all previous works). The errors in the data shown in figures 8–10 are comparable to the thickness of the lines. As expected, C_{kk} decreases as y gets larger, while C_{bb} increases. Thus we can safely say that

$$C_{kk} \rightarrow \text{const} \quad \text{for } N \rightarrow \infty, \quad (20)$$

since this was already shown for $y = 2$. The scaling of C_{bb} is much more subtle. Previous analyses, starting with the seminal work of [16], obtained $C_{bb} \sim N^{2\phi-1}$ with $\phi \approx 0.6$ to 0.65. Just making least square fits to the curves in figure 9 for the largest values of y would give the same estimate. But we think that this is misleading, as it was also for $y \leq 2$. First of all, we would expect some sort of crossover in figure 9, which is not seen: the transition from $y = 2$ to $y > 2$ is perfectly smooth. Secondly, we should expect C_{kk} and C_{bb} to scale in the same way. These two variances control the divergence of $Z_N(y, \tau)$ as we cross the transition curve vertically and horizontally. In both cases one crosses the transition curve *transversally*, and along each transverse line the divergence should be the same. Therefore we suggest that $C_{bb} \sim \text{const}$, i.e., $\phi = 1/2$.

6. Collapsed animals: one or two phases?

According to [9, 10, 22] there are indeed two collapsed phases (one rich in contacts, the other rich in bonds). The transition line between them bifurcates off from the collapse curve not at $y = y_c = 2$, but at $y^* \approx 4$ (see the figure shown in [7]). If this is basically true, but with $y^* \approx 3.2$, this would easily explain our results discussed in the previous section: the point (y^*, τ^*) would separate an intermediate part $2 < y \leq y^*$ of the collapse curve which is still basically contact driven from the bond-driven part $y > y^*$. The only unusual feature would be that the fixed point (y^*, τ^*) has to be attractive when approached from the left along the collapse transition curve, while it has to be repulsive on the right. Such a behaviour is not typically expected from the RG group, although we see no reason why it should be forbidden (it requires that the linearized RG flow near the fixed point is zero, and the flow is dominated by quadratic terms).

For a direct test of this scenario, one has to simulate deep in the collapsed region and verify that there is a transition between two different collapsed phases. To search for such a transition, we have to modify our strategy. We cannot use the gyration radius as an indicator (because $R_N^2 \sim N$ in both phases), and we cannot use the partition sum either. We checked that the free energy of collapsed animals has a surface term, $\ln Z_N = N \ln \mu - \text{const} N^{1/2} + \dots$, as one expects for any two-dimensional compact object (a similar term is well known for droplets, and was shown to exist also for collapsed unbranched polymers [29, 30]). Even if there is in addition a term $\sim \ln N$ in the free energy, there would be just too many unknown parameters to pin it down precisely and to use this for locating the transition.

Thus we have to look directly to the order parameter, which is the difference $b - k$, and its fluctuations². In figure 15 we show the normalized average difference $\langle k - b \rangle / N$ between the numbers of contacts and bonds against τ , for several values of N . More precisely, we used $b - N + 1$ instead of b in this figure, which is the number of bonds exceeding the minimal number. For this figure, y was kept fixed at $y = 3.75$, i.e., we scan figure 1 along a vertical line which starts at the collapse transition line at a τ which the previous section suggested to be above τ^* . We see that this difference increases with τ , indicating that we move indeed from a situation rich in bonds to a system rich in contacts. But this increase is so smooth that this cannot be used as an argument in favour of a

² Define a spin variable $s_i = 1$ if the edge i between two occupied adjacent lattice sites is occupied by a bond, and $s_i = -1$ if it is occupied by a contact. We could then have also looked at spatial spin-spin correlations, but we shall not discuss this further in the present paper.

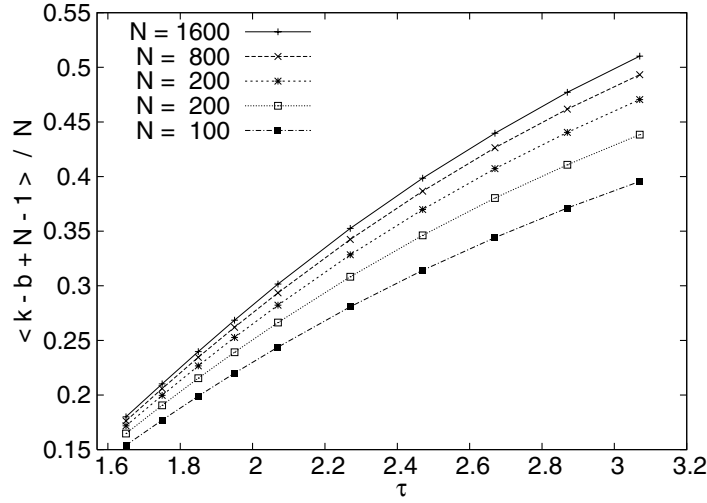


Figure 15. Normalized average differences $(k - b')/N$ at $y = 3.75$ plotted against τ , for $N = 100, 200, 400, 800$, and 1600 (from bottom to top). Here, $b' = b - N + 1$ is the number of bonds exceeding the minimal number needed for the cluster to be connected. Error bars are much smaller than the size of the symbols.

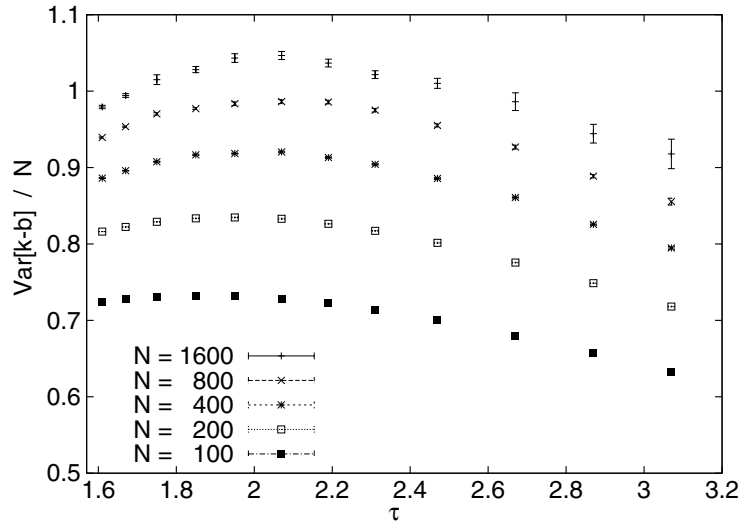


Figure 16. Analogous to figure 15, but showing the normalized variances $C_{k-b, k-b}$.

thermodynamic phase transition. Instead, figure 15 could suggest that there is no such transition. But we should be aware that an analogous search for the θ collapse in ordinary (unbranched) polymers, based on the number of contacts, would also fail, because this number varies rather smoothly with temperature [31]. Thus we would need much larger systems to obtain a firm conclusion from a plot like in figure 15.

Things change if we look at the corresponding variances; see figure 16. If there is a phase transition, we expect a peak which becomes higher as N increases. What we see

is not quite a sharp peak (it is rather a broad bump), but its height definitely increases with N . Also, its maximum shifts with increasing N to higher values of τ , indicating that it is not related to the collapse transition. Notice that the existence of this bump and its increase with N are definitely not due to any statistical fluctuations.

It is not clear whether the data shown in figures 15 and 16 taken by themselves speak more for or against a phase transition between two collapsed phases. They certainly do not exclude this possibility. And taken together with the anomaly found in the previous section, we believe that such a transition is the most natural interpretation. In this case, a naive (least square, say) fit to an ansatz $C_{k-b,k-b} \sim N^{2\phi-1}$ would suggest $\phi \approx 0.54$, but there is the same kind of curvature in plots of $C_{k-b,k-b}$ versus $\ln N$ as in figures 8 and 9, and a more careful extrapolation suggests again that ϕ is close to $1/2$; more precisely, $\phi = 0.52 \pm 0.02$. Since the shift of the maximum to larger τ with increasing N seems to stop for $N > 400$, we locate the transition near the maximum observed for $N = 1600$, $\tau \approx 2.1 \pm 0.2$. Because these simulations were very costly in terms of CPU time, we have not made similar searches at different values of y , and the location of the transition line indicated in figure 1 should only be taken as a very rough guess.

We should however point that it seems hard to come up with a theoretical argument for such a transition. Usually, a phase transition requires some sort of cooperativity, i.e., some mechanism leading to positive correlations. In the ferromagnetic Ising model, for example, this is the spin–spin interaction which tends to make neighbouring spins parallel. In the antiferromagnetic Ising model on a square lattice, the spin–spin interaction favours parallel next-nearest neighbours. In the present case we see no such interactions. The only source for correlations is the fact that the bonds must make the cluster connected, i.e., they cannot all be in one part of the cluster, leaving the rest of the cluster to contacts. But this should give rise to negative correlations, and it is not clear how it can lead to a phase transition.

We should also mention that the individual bond and contact variances show no bump or peak when going into the collapsed region, but fall off continuously with τ . The bump seen in the variance of $k - b$ is entirely due to an increase of the absolute value of the covariance. Indeed, as we move off the collapse curve into the collapsed phase, the scaling of C_{kb} changes from decreasing with N to increasing with it, and continues to increase with N even for very large τ .

7. Conclusions

We have presented extensive Monte Carlo simulations of collapsing lattice animals and collapsing lattice trees. We used a novel algorithm which should be most efficient near the (bond) percolation point, and it indeed was. At the percolation point it was even more efficient than the straightforward Leath algorithm. It was also very efficient along the entire transition line for $y < 2$, including the point $y = 0$ which describes the collapse of weakly embeddable trees. For the latter we conjectured exact values for all critical exponents.

Our simulations encountered severe problems for the bond-induced collapse at $y > 2$. For very large y , near the point studied first by Derrida and Herrmann, it essentially breaks down. Thus we were able to verify their analysis, but we were not able to improve on it.

For moderately large y , i.e., for $3.5 \leq y \leq 4.0$, our algorithm is still efficient enough to generate high statistics samples of rather large clusters ($N \approx 1000$). But we found there very large corrections to scaling which prevent us from extracting precise values of the critical exponents, and we can only give upper bounds for ν and θ : $\nu < 0.515, \theta < 2.0$. These corrections seem to be absent for even smaller y (i.e., $2.5 \leq y \leq 3.0$), but we cannot of course exclude that they would show up if we would go to even larger clusters. Assuming this not to happen, we can then propose $\nu = 0.5220 \pm 0.0004, \phi = 0.5$ and $\theta = 2.12 \pm 0.01$ along the bond-induced collapse transition, while $\nu = 37/69 \approx 0.53623, \phi = 0.5$ and $\theta = 59/32 = 1.84375$ for collapsing trees. Together with the exact results $\nu = 48/91 \approx 0.52747, \phi = 1/2$, and $\theta = 187/91 \approx 2.054945$ for critical percolation, these values show that there are indeed (at least) three different universality classes. We cannot rule out that the anomalies observed at $y \approx 3.75$ hint at yet another universality class.

We found somewhat weaker but still statistically significant evidence for a transition between two collapsed phases, one contact rich and the other bond rich. This line branches off from the collapse line at $y^* = 3.2 \pm 0.2$, which is clearly larger than the value $y = 2$ for critical percolation, but is substantially smaller than the estimate $y^* \approx 4$ given in [9, 10, 22]. The crossover exponent at this transition is again $\phi \approx 0.5$. Other critical exponents were not measured for this transition.

We should finally comment on our claim that $\phi = 1/2$ for critical percolation (and indeed along the entire collapse line and for the transition between the two collapsed phases). This is based on the definition of ϕ in terms of bond and/or contact fluctuations. It is also true for site percolation, if we look at fluctuations in the number of non-wetted surface sites. It should not be confused with the fact that the crossover exponent in a scaling ansatz, equation (9), usually called σ in the percolation literature, is smaller than $1/2$. From this scaling ansatz it follows surprisingly that the variances of bond and contact numbers must scale $\sim N$. Our claim that $\phi = 1/2$ is entirely based on this observation, and is made in spite of the fact that naive fits would give $\phi > 1/2$. This should again be a warning that power law fits not guided by a solid theory can be very misleading.

Acknowledgment

It is a pleasure to thank Walter Nadler for numerous discussions and for critically reading the manuscript.

References

- [1] Stauffer D and Aharony A, 1992 *Introduction to Percolation Theory* 2nd edn (London: Taylor and Francis)
- [2] Fortuin C M and Kasteleyn P W, 1972 *Physica* **57** 536
- [3] Swendsen R H and Wang J-S, 1986 *Phys. Rev. Lett.* **57** 2607
- [4] Lubensky T C and Isaacson J, 1978 *Phys. Rev. Lett.* **41** 829
Lubensky T C and Isaacson J, 1979 *Phys. Rev. Lett.* **42** 410 (erratum)
Lubensky T C and Isaacson J, 1979 *Phys. Rev. A* **20** 2130
- [5] de Gennes P G, 1979 *Scaling Concepts in Polymer Physics* (Ithaca, NY: Cornell University Press)
- [6] Grosberg A Yu and Khokhlov A R, 1994 *Statistical Physics of Macromolecules* (New York: AIP)
- [7] Henkel M and Seno F, 1996 *Phys. Rev. E* **53** 3662
- [8] Seno F and Vanderzande C, 1994 *J. Phys. A: Math. Gen.* **27** 5813
Seno F and Vanderzande C, 1994 *J. Phys. A: Math. Gen.* **27** 7937
- [9] Flesia S, Gaunt D S, Soteris C E and Whittington S G, 1994 *J. Phys. A: Math. Gen.* **27** 5831
- [10] Flesia S, Gaunt D S, Soteris C E and Whittington S G, 1992 *J. Phys. A: Math. Gen.* **25** L1169

- [11] Stratychuk L M and Soteros C E, 1996 *J. Phys. A: Math. Gen.* **29** 7067
- [12] Madras N and Janse van Rensburg E J, 1997 *J. Stat. Phys.* **86** 1
- [13] Janse van Rensburg E J and Madras N, 1997 *J. Phys. A: Math. Gen.* **30** 8035
- [14] Janse van Rensburg E J, Orlandini E and Tesi M C, 1999 *J. Phys. A: Math. Gen.* **32** 1567
- [15] Janse van Rensburg E J, 2000 *J. Phys. A: Math. Gen.* **33** 3653
- [16] Derrida B and Herrmann H J, 1983 *J. Physique* **44** 1365
- [17] Dickman R and Schieve W C, 1984 *J. Physique* **45** 1727
- [18] Lam P M, 1987 *Phys. Rev. B* **36** 6988
- [19] Lam P M, 1988 *Phys. Rev. B* **38** 2813
- [20] Chang I S and Shapir Y, 1988 *Phys. Rev. B* **38** 6736
- [21] Nienhuis B, cited in [8]
- [22] Peard P, 1995 *PhD Thesis* King's College, London
- [23] Hsu H-P, Nadler W and Grassberger P, 2005 *J. Phys. A: Math. Gen.* **38** 775
- [24] Grassberger P, 1997 *Phys. Rev. E* **56** 3682
- [25] Leath P, 1976 *Phys. Rev. B* **14** 5046
- [26] Borstnik B and Lukman D, 2000 *Euro. Phys. J. B* **16** 113
- [27] Grassberger P, Sutter P and Schäfer L, 1997 *J. Phys. A: Math. Gen.* **30** 7039
- [28] Grassberger P, 2005 *J. Phys. A: Math. Gen.* **38** 323
- [29] Owczarek A L, Prellberg T and Brak R, 1993 *Phys. Rev. Lett.* **70** 951
- [30] Hsu H P and Grassberger P, 2002 *J. Phys. A: Math. Gen.* **35** L759
- [31] Grassberger P and Hegger R, 1995 *J. Chem. Phys.* **102** 6881